室蘭工業大学
学術資源アーカイブ
Muroran Institute of Technology Academic Resources Archive

Sensitivity-Based Structural Optimal Design With Bi-Directional Beam Propagation Method for Photonic Devices in High-Index-Contrast Waveguides

メタデータ	言語: English 出版者: IEEE-INST ELECTRICAL ELECTRONICS ENGINEERS INC 公開日: 2020-12-23 キーワード (Ja): キーワード (En): High-index-contrast waveguide, sensitivity analysis, structural optimization, Bi-directional beam propagation method (Bi-BPM) 作成者: 井口, 亜希人, 森本, 佳太, 辻, 寧英 メールアドレス: 所属:
URL	http://hdl.handle.net/10258/00010349

IEEE Photonics Journal
An IEEE Photonics Society Publication

Open Access

Sensitivity-Based Structural Optimal Design With Bi-Directional Beam Propagation Method for Photonic Devices in High-Index-Contrast Waveguides

Volume 12, Number 5, October 2020

Akito Iguchi, ***Member, IEEE***
Keita Morimoto, ***Student Member, IEEE***
Yasuhide Tsuji, ***Senior Member, IEEE***

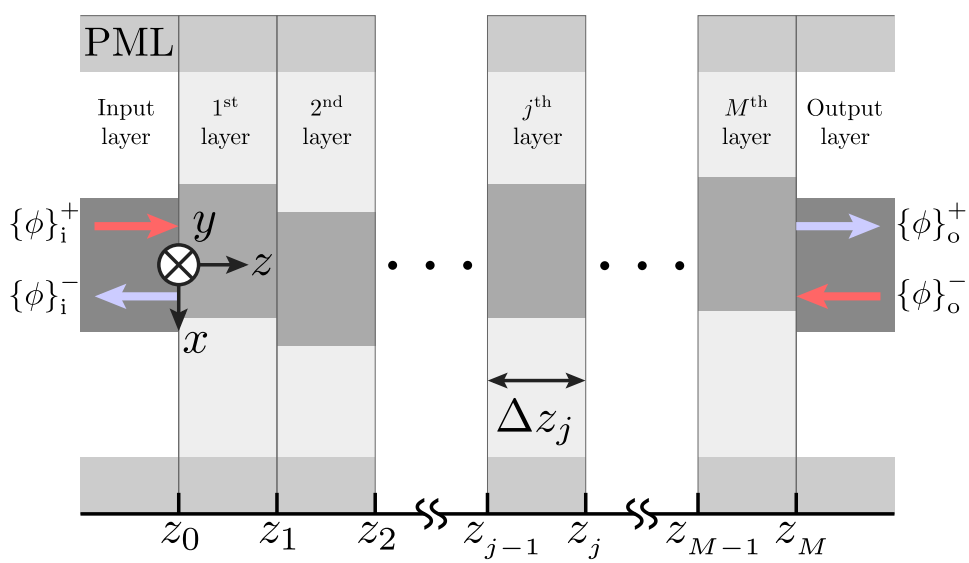

DOI: 10.1109/JPHOT.2020.3029032

Sensitivity-Based Structural Optimal Design With Bi-Directional Beam Propagation Method for Photonic Devices in High-Index-Contrast Waveguides

Akito Iguchi, ***Member, IEEE***,
Keita Morimoto, ***Student Member, IEEE***,
and Yasuhide Tsuji, ***Senior Member, IEEE***

Department of Engineering, Muroran Institute of Technology, Muroran 050-8585, Japan

DOI:10.1109/JPHOT.2020.3029032
This work is licensed under a Creative Commons Attribution 4.0 License. For more information, see https://creativecommons.org/licenses/by/4.0/

Manuscript received July 7, 2020; revised August 25, 2020; accepted October 2, 2020. Date of publication October 7, 2020; date of current version October 21, 2020. This work was supported by JSPS KAKENHI under Grant JP 20K22408. Corresponding author: Akito Iguchi. (e-mail: iguchia@mmm.muroran-it.ac.jp).

Abstract: This paper presents structural optimization based on sensitivity analysis exploiting a bi-directional beam propagation method (Bi-BPM) to design efficiently passive components in high-index-contrast optical waveguides. In this study, the Bi-BPM based on scaled-version Denman-Beavers iteration (S-DBI) with branch-cut technique, and scattering operator formulation (SO-Bi-BPM) is employed to execute stable, accurate wave-propagation analysis. Comparing three computation approaches of sensitivity with respect to design variables, efficient way of sensitivity analysis is revealed when the SO-Bi-BPM is used. The application range of the presented design approach is studied by designing a wavelength filter with waveguide grating, and a polarizer based on 1D photonic crystal (1D-PhC).

Index Terms: High-index-contrast waveguide, sensitivity analysis, structural optimization, Bi-directional beam propagation method (Bi-BPM).

1. Introduction

Miniaturization of integrated photonic devices is intensively studied in recent years to achieve lower power consumption and higher speed optical network systems. In particular, optical components in silicon on insulator (SOI) platform, and plasmonics have attracted attention because of strong confinement of lightwave in core region [1], [2]. As a means of enhancement of its performance, structural optimization based on iteration of numerical simulations is widely applied to design of small-footprint and high-performance optical components [3]–[7]. A finite-difference time-domain (FDTD) method, its frequency domain method (FDFD), a finite element method (FEM), or a beam propagation method (BPM) have been widely used as a numerical simulation technique, and they have already had wide variety of achievement in design of optical waveguide components [3]–[9]. The BPM based on a slowly varying envelope approximation (SVEA) is very efficient technique, but it may be difficult to apply generally to design of components in high-index-contrast waveguides such as SOI devices. Although the FDTD and the FEM can be employed for general design of optical components, it is well known that they require much intensive computational resources.

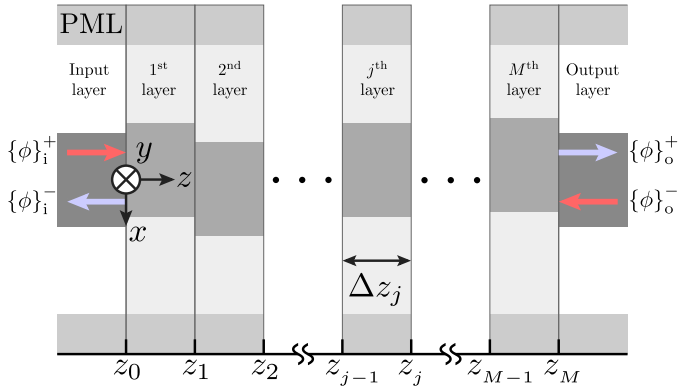

Fig. 1. A 2-D multi-layered waveguide consists of homogeneous layers in *z*-direction.

We presented shape and topology optimization utilizing the standard BPMs based on sensitivity analysis to achieve efficient design of photonic integrated components [10]–[12]. However, these design approaches cannot be applied versatilely to design of optical components in high-index-contrast waveguides due to limitation of the SVEA. So far, modal-based methods [13]–[16] and field-based methods also known as the bidirectional beam propagation methods (Bi-BPM) [17]–[22] which overcome drawbacks of the standard BPM have been developed. Modal-based methods have been well studied, and these methods are applied to waveguide discontinuity problems [13]–[16]. Although modal-based techniques can reduce matrix dimension, computational cost may be high to analyze accurately propagation behavior in versatile strong discontinuity problems because a sufficiently large number of eigenpairs has to be computed [21], [22]. The Bi-BPMs can take into account wider range of scattering and propagating waves including backward scattering by computing accurately square root of characteristic matrix. Recently, rigorous and efficient ways of computing the square root of matrix are reported [18], [21], thus, this method may be promising technique to deal with versatile 2-D approximated and 3-D design problems. In the Bi-BPMs, transmission and reflection fields are computed by transmission operator [17], [18] or scattering operator [19]–[21] in whole system. These techniques can analyze periodic components efficiently doubling the operator of a periodic system.

This paper presents approaches of structural optimization utilizing the Bi-BPM for design of photonic integrated components, and studies these application. In this study, a scattering-operator-based Bi-BPM (SO-Bi-BPM) are employed because of numerical stability. The Bi-BPM has characteristic that square root of a characteristic matrix is computed by approximated or direct methods. In recent study of the Bi-BPM, the Denman-Beavers iteration (DBI) have been employed to compute the square root of matrix, and the efficiency is reported. We employ in this study its scaled scheme, a scaled-version DBI (S-DBI) to reduce the DB iteration count. In the structural optimization with high design flexibility, gradient-based algorithms are widely used to search design variable space. Gradient-based methods such as a steepest descent method require computation of sensitivity with respect to design variables. This paper offers three design approaches based on sensitivity analysis when the SO formulation is employed. These design approaches are compared in 2-D approximated design of a waveguide reflector and polarizer based on 1-D photonic crystal, and usefulness of presented design approaches are studied.

2. Sensitivity Analysis With Bi-Directional BPM

2.1. Bi-Directional BPM Based on Scattering Operator

We consider a 2-D multi-layered waveguide which consists of homogeneous layers in *z*-direction shown in Fig. 1. The 2-D Helmholtz equation in a homogeneous layer truncated by the perfectly

matched layer (PML) can be written as follows [18]:

$$\frac{\partial^2\phi(x,z)}{\partial z^2}+\frac{1}{p(x)s_x(x)}\frac{\partial}{\partial x}\left\{\frac{p(x)}{s_x(x)}\frac{\partial\phi(x,z)}{\partial x}\right\}+k_0^2n^2(x)\phi(x,z)=0 \tag{1}$$

$$\phi(x,z)=\begin{cases}E_y(x,z)\\H_y(x,z)\end{cases},\ p(x)=\begin{cases}1 & \text{[for TE wave]}\\1/n^2(x) & \text{[for T wave]}\end{cases} \tag{2}$$

where k_0 is a wavenumber in free space, and $n(x)$ is refractive index distribution. s_x is a stretching parameter of complex coordinate in the PML, and is defined by

$$s_x(x)=\begin{cases}1-j\left(\frac{x-x_{\mathrm{L}}}{d_{\mathrm{PML}}}\right)^{\alpha}\tan\delta & [x<x_{\mathrm{L}}]\\1-j\left(\frac{x_{\mathrm{R}}-x}{d_{\mathrm{PML}}}\right)^{\alpha}\tan\delta & [x_{\mathrm{R}}<x]\\1 & [x_{\mathrm{L}}\le x\le x_{\mathrm{R}}]\end{cases} \tag{3}$$

where x_{L} and x_{R} ($x_{\mathrm{L}}<x_{\mathrm{R}}$) are surface positions between the computational window and the PML, d_{PML} is its thickness, and $\tan\delta$ is a loss tangent at a terminal position of the PML. In this study, $\alpha=2$ is chosen. Matrix-vector form of (1) is written as follows:

$$\frac{\partial^2\{\phi\}}{\partial z^2}+[Q]\{\phi\}=0 \tag{4}$$

where $\{\phi\}$ is a vector form of transversal electro-magnetic field, and $[Q]$ is a characteristic matrix representing the operator, $[p\partial/\partial x(p\partial/\partial x)+k_0^2n^2]$. The improved finite difference scheme with second-order (IFD2) [23] is applied to the operator in this study. The solution of (4) in the j-th layer can be expressed by [18]

$$\{\phi\}=\exp\left[-j\sqrt{[Q]_j}\,(z-z_{j-1})\right]\left\{\phi^+(z_{j-1}^+)\right\}+\exp\left[j\sqrt{[Q]_j}(z-z_j)\right]\left\{\phi^-(z_j^-)\right\}. \tag{5}$$

$\{\phi^+(z)\}$ and $\{\phi^-(z)\}$ indicate forward and backward propagating fields, and $j=\sqrt{-1}$.

In the scattering operator approach, following scattering matrix is constructed [19], [20]:

$$\begin{Bmatrix}\{\phi\}_{\mathrm{i}}^-\\\{\phi\}_{\mathrm{o}}^+\end{Bmatrix}=\left[\begin{bmatrix}S_{11}(z_0^-)\\S_{21}(z_0^-)\end{bmatrix}\begin{bmatrix}S_{12}(z_M^+)\\S_{22}(z_M^+)\end{bmatrix}\right]\begin{Bmatrix}\{\phi\}_{\mathrm{i}}^+\\\{\phi\}_{\mathrm{o}}^-\end{Bmatrix}. \tag{6}$$

$\{\phi\}_{\mathrm{i}}^+$ and $\{\phi\}_{\mathrm{o}}^-$ are input fields into the waveguide system at the input and output waveguides, and $\{\phi\}_{\mathrm{i}}^-$ and $\{\phi\}_{\mathrm{o}}^+$ are output ones. $[S_{11}(z)]$ and $[S_{21}(z)]$ ($[S_{12}(z)]$ and $[S_{22}(z)]$) indicate scattering matrices of a system ranging from z to z_M^+ (z_0^- to z).

Propagating fields of adjacent layers can be correlated with each other using (5) and continuity of ϕ and $p\partial\phi/\partial z$. A procedure to compute scattering matrix can be derived by the relation of propagating fields and the definition of scattering operator. The sequential procedure to compute the "forward" components of the scattering matrix, $[S_{11}(z_0^-)]$ and $[S_{21}(z_0^-)]$, is shown as follows [19]:

1) $[S_{11}(z_M^+)]=[0]$, $[S_{21}(z_M^+)]=[I]$, where $[I]$ is the identity matrix.
2) For $j=M,\ldots,0$, do
   a) $[C]_j=[Z]_j^{-1}[Z]_{j+1}([I]-[S_{11}(z_j^+)])([I]+[S_{11}(z_j^+)])^{-1}$, where $[Z]_j\equiv[p]_j\sqrt{[Q]_j}$.
   b) $[S_{11}(z_j^-)]=([I]+[C]_j)^{-1}([I]-[C]_j)$.
   c) $[S_{21}(z_j^-)]=[S_{21}(z_j^+)]([I]+[S_{11}(z_j^-)])^{-1}([I]-[S_{11}(z_j^-)])$.
   d) If $j\neq 0$, then $[S_{11}(z_{j-1}^+)]=[P]_j[S_{11}(z_j^-)][P]_j$, $[S_{21}(z_{j-1}^+)]=[S_{21}(z_j^+)][P]_j$, where $[P]_j\equiv\exp[-j\sqrt{[Q]_j}\Delta z_j]$, $\Delta z_j\equiv z_{j-1}-z_j$.

$[p]$ indicates a diagonal matrix consists of transversal distribution of $p(x)$ in (2). The "backward" ones, $[S_{12}(z_M^+)]$ and $[S_{22}(z_M^+)]$, can be constructed in the same fashion. As shown in the above procedure, the square root of matrix and exponential matrix in all homogeneous layers have to be evaluated.

In order to compute square root of $[Q]$ stably, a branch-cut technique is employed in Bi-BPMs [18], [21]: $[Q']\equiv[Q]\exp(-j\theta)$, where $\theta\in]0,\pi[$ is a rotation angle. In this study, we employ scaled-version Denman-Beavers Iteration (S-DBI) scheme to efficiently compute the square root of $[Q']$ [24]:

1) $[X]_0 = [Q']$, $[Y]_0 = [I]$.
2) Until stop criteria is satisfied, for $n = 0, 1, 2, \cdots$, do
   a. $\nu_n = |\det[X]_n \det[Y]_n|^{-1/(2N)}$, where N is dimension of matrix.
   b. $[X]_{n+1} = (\nu_n [X]_n + \nu_n^{-1} [Y]_n^{-1})/2$.
   c. $[Y]_{n+1} = (\nu_n [Y]_n + \nu_n^{-1} [X]_n^{-1})/2$.

If $n \to \infty$, $[X] \to \sqrt{[Q']}$ and $[Y] \to (\sqrt{[Q']})^{-1}$. Eventually, the square root of $[Q]$ is obtained by $\sqrt{[Q]} = \sqrt{[Q']}\exp(j\theta/2)$. In the DB iteration, inverse matrix is computed twice at each iteration. The determinant can be easily obtained by multiplying diagonal elements of $[L]$ or $[U]$ in LU-decomposition to compute an inverse matrix. By multiplying the scaling factor, ν, by $[X]$ and $[Y]$, faster convergence can be expected compared to the standard DBI. In the procedure to construct scattering matrix, inverse of $\sqrt{[Q]}$ is required at each iteration. It is one motivation to use the DBI that the $\sqrt{[Q]}$ and its inverse matrix are simultaneously obtained.

Using the computed square root of $[Q]$, a exponential matrix, or a propagator $[P]$ can be calculated. In this study, Padé (r,s) approximation is employed to compute it. To improve approximation accuracy, the approximation is applied to $[P'] \equiv [P]\exp(jk_0 n_0 \Delta z)$ [18], [25]:

$$[P'] \approx [D(r,s)]^{-1}\,[N(r,s)] \tag{7}$$

$$[N(r,s)] = \sum_{n=0}^{r} \frac{(r+s-n)!r!}{(r+s)!n!(r-n)!}\left[-j\left(\sqrt{[Q]} - k_0 n_0 [I]\right)\Delta z\right]^n \tag{8}$$

$$[D(r,s)] = \sum_{n=0}^{s} \frac{(r+s-n)!s!}{(r+s)!n!(s-n)!}\left[j\left(\sqrt{[Q]} - k_0 n_0 [I]\right)\Delta z\right]^n \tag{9}$$

where n_0 is a reference refractive index. Eventually, the original propagator is obtained by $[P] = [P']\exp(-jk_0 n_0 \Delta z)$.

The other approach to construct the whole scattering matrix is to joint local scattering matrices using Redheffer's star (RS) product [26]. The global scattering matrix, $[S]_{\mathrm{G}}$, can be constructed by connecting local scattering matrices, $[S]_j$ at each layer using RS product:

$$[S]_{\mathrm{G}} = [S]_{\mathrm{in}} \star [S]_1 \star [S]_2 \star \cdots \star [S]_M \star [S]_{\mathrm{out}} \tag{10}$$

where $\star$ denotes RS product defined as

$$\left[\begin{bmatrix} S_{11(\mathrm{A+B})} \\ S_{21(\mathrm{A+B})} \end{bmatrix} \begin{bmatrix} S_{12(\mathrm{A+B})} \\ S_{22(\mathrm{A+B})} \end{bmatrix}\right] = \left[\begin{bmatrix} S_{11(\mathrm{A})} \\ S_{12(\mathrm{A})} \end{bmatrix} \begin{bmatrix} S_{12(\mathrm{A})} \\ S_{22(\mathrm{A})} \end{bmatrix}\right] \star \left[\begin{bmatrix} S_{11(\mathrm{B})} \\ S_{21(\mathrm{B})} \end{bmatrix} \begin{bmatrix} S_{12(\mathrm{B})} \\ S_{22(\mathrm{B})} \end{bmatrix}\right] \tag{11}$$

with

$$\left[S_{11(\mathrm{A+B})}\right] = \left[S_{11(\mathrm{A})}\right] + \left[S_{12(\mathrm{A})}\right]\left([I] - \left[S_{11(\mathrm{B})}\right]\left[S_{22(\mathrm{A})}\right]\right)^{-1}\left[S_{11(\mathrm{B})}\right]\left[S_{21(\mathrm{A})}\right] \tag{12}$$

$$\left[S_{12(\mathrm{A+B})}\right] = \left[S_{12(\mathrm{A})}\right]\left([I] - \left[S_{11(\mathrm{B})}\right]\left[S_{22(\mathrm{A})}\right]\right)^{-1}\left[S_{12(\mathrm{B})}\right] \tag{13}$$

$$\left[S_{21(\mathrm{A+B})}\right] = \left[S_{21(\mathrm{B})}\right]\left([I] - \left[S_{22(\mathrm{A})}\right]\left[S_{11(\mathrm{B})}\right]\right)^{-1}\left[S_{21(\mathrm{A})}\right] \tag{14}$$

$$\left[S_{22(\mathrm{A+B})}\right] = \left[S_{22(\mathrm{B})}\right] + \left[S_{21(\mathrm{B})}\right]\left([I] - \left[S_{22(\mathrm{A})}\right]\left[S_{11(\mathrm{B})}\right]\right)^{-1}\left[S_{22(\mathrm{A})}\right]\left[S_{12(\mathrm{B})}\right]. \tag{15}$$

Local scattering matrices, $[S]_j$ $(j = 1, \ldots, M)$, and those of input and output waveguide, $[S]_{\mathrm{in}}$, $[S]_{\mathrm{out}}$, can be computed independently.

In this paper, we assume that a waveguide system contains a periodic waveguide, and two approaches to compute global scattering matrix are considered. We call tentatively the first approach a "sweeping" approach:

$$[S]_{\mathrm{G}} = [S]_{\mathrm{in}} \star P_{N_r}\left([S]_{1,M}\right) \star [S]_{\mathrm{out}} \tag{16}$$

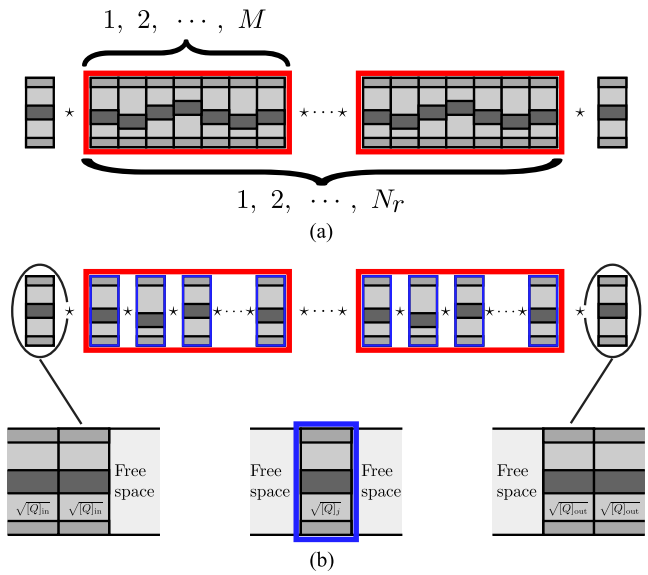

Fig. 2. Concept schematics of (a) a sweeping approach and (b) a dividing approach.

with

$$P_{N_r}([S]) = \underbrace{[S] \star [S] \star \cdots \star [S]}_{(N_r-1)\text{ times RS product}}. \tag{17}$$

A concept schematic is shown in Fig. 2(a). $P_{Nr}([S])$ can be computed using a doubling process efficiently [20], [27]. In this approach, $[S]_{1,M}$, which is a scattering matrix of a system from 1-st to M-th layer, is computed by the sequential process. The second approach is called a "dividing" approach:

$$[S]_{\mathrm{G}} = [S]_{\mathrm{in}} \star P_{N_r}\left([S]_1 \star [S]_2 \star \cdots \star [S]_M\right) \star [S]_{\mathrm{out}}. \tag{18}$$

In this approach, first, local scattering matrices are computed, then $[S]_{1,M}$ are constructed by connecting them with RS product. The j-th local system is constructed by j-th homogeneous layer sandwiched between free space, and that of input or output waveguides, $[S]_{\mathrm{in}}$ or $[S]_{\mathrm{out}}$, is composed as shown in shown in Fig. 2(b). Additional operations are required in the dividing approach. Nevertheless, if design variables are distributed locally, it is expected that sensitivity analysis is more efficiently conducted because local scattering matrices can be computed parallelly and an interim scattering matrix can be utilized. In the next subsection, three approaches to compute sensitivity with respect to design variables are shown.

2.2. Sensitivity Analysis

In structural optimization, determining an objective function to express device performance, the performance is maximized by solving minimization problem of the objective function. To solve a minimization problem, gradient methods based on sensitivity analysis are widely used. We let $f(\{a\})$ objective function where $\{a\}$ is a vector of design variables. In the gradient methods, the variable space is searched based on sensitivity of $f(\{a\})$ with respect to design variables. In this paper, forward FD is used to evaluate the sensitivity:

$$\frac{\partial f(\{a\})}{\partial a_n} \approx \frac{f(\{a\} + \Delta\{e\}_n) - f(\{a\})}{\Delta} \tag{19}$$

where a_n is a n-th design variable, Δ is an arbitrary small value, and $\{e\}_n$ is a unit vector in the searching space. If a design variable is localized only in the j-th layer, calculation of a perturbed $\sqrt{\{Q\}_j}$ is required to compute $f(\{a\} + \Delta\{e\}_n)$, and a perturbed $[S]_{\mathrm{G}}$.

In the sweeping approach, the sequential procedure has to be conducted again. Although the dividing approach requires not only the perturbed $\sqrt{\{Q\}_j}$ but also a perturbed local scattering matrix, the perturbed $[S]_{\mathrm{G}}$ can be computed only by the RS product using calculated local scattering matrices:

$$[\tilde{S}]_{\mathrm{G}} = [S]_{\mathrm{in}} \star P_{N_r}\left([S]_1 \star \cdots \star [\tilde{S}]_j \star \cdots \star [S]_M\right) \star [S]_{\mathrm{out}} \tag{20}$$

where $[\tilde{S}]$ denotes a perturbed scattering matrix. We call an optimal design using this sensitivity analysis approach a dividing approach A. If interim scattering matrices of the RS product are stored in the first analysis, $[\tilde{S}]_{\mathrm{G}}$ can be computed more efficiently by

$$[\tilde{S}]_{\mathrm{G}} = [S]_{\mathrm{in}} \star P_{N_r}\left([S]_{1,j-1} \star [\tilde{S}]_j \star [S]_{j+1,M}\right) \star [S]_{\mathrm{out}} \tag{21}$$

with

$$[S]_{n,m} = [S]_n \star [S]_{n+1} \star \cdots \star [S]_{m-1} \star [S]_m \quad [n < m]. \tag{22}$$

Although this approach requires additional computational resources to store $[S]_{1,j}$ and $[S]_{j,M}$ ($j = 1, \ldots, M$), it can be expected that elapsed time of optimal design are saved by reducing computational time of sensitivity analysis. We call this optimal design approach a dividing approach B. The flow charts of the three approaches are shown in Fig. 3. The process to compute $\sqrt{[Q]_j}$, the local scattering matrix $[S]_j$, and sensitivity is implemented parallelly using OpenMP. In the next section, these approaches are compared by designing specific optical devices.

3. Application Examples

3.1. Reflector Based on Waveguide Grating

First design example is a reflector as shown in Fig. 4. In this example, waveguide reflector based on grating with $(n + 0.5)$ periods is designed by optimizing core widths. The refractive indices of core (Si) and cladding (SiO_2) materials are determined by an equation (22) in [28] and a Sellmeier equation in [29], respectively. These indices at central wavelength of 1.55 μm are about 3.475 and 1.444, respectively. The objective function is determined as follows so that a fundamental TE wave (TE_0) is launched into port 1 and the wave is totally reflected.

$$\underset{\{a\}}{\text{minimize}} \quad f(\{a\}) = \sum_{\lambda \in \{L\}} \left[\left\{1 - P_{\mathrm{refl}}(\{a\}, \lambda)\right\}^2 + \left\{0 - P_{\mathrm{thru}}(\{a\}, \lambda)\right\}^2\right] \tag{23}$$

where $\{a\} = \{w_1, w_2, \ldots, w_{2n+1}\}$ is a vector of design variables, P_{refl} and P_{thru} are normalized reflected power of TE_0 wave at input port and transmitted power at through port. $\{L\}$ is a set of wavelengths taken into account in this example, and here three wavelengths are considered to achieve wider wavelength range of operation: $\{L\} = \{1.5,\ 1.55,\ 1.6\ \mu\mathrm{m}\}$. The other structural parameters shown in Fig. 4 are let to be as follows: $w_{\mathrm{io}} = 400$ nm, $l_{\mathrm{io}} = 100$ nm, $\Lambda = 260$ nm (duty ratio is 0.5). Transversal computational window size with the PML is 5 μm, and the number of sampling points is 250. The PML thickness is let to be 500 nm. Initial design variables are $w_{2m+1} = 0.4\ \mu$m ($m = 0, 1, \ldots, n$), $w_{2\,m} = 0.2\ \mu$m ($m = 1, 2, \ldots, n$).

The results of optimization when $n = 10$ are shown in Fig. 5. Figure 5 (a) is value of the objective function as a function of iteration number. Insets are the initial profile and optimized one after 1000 iterations. Figure 5 (b) shows transmittance and reflectance spectra of the initial and the optimized reflector. The optimized reflector achieves lower-loss and higher-reflectance compared with the initial profile. The optimized profile has > -0.055 dB insertion loss and transmittance of < -20 dB at wavelength range from 1.5 to 1.574 μm covering C-band. For visualization, propagating fields in the optimized reflector computed by the FDTD are shown in Fig. 5 (c). We can see that reflector is surely worked as the results of the Bi-BPM analysis.

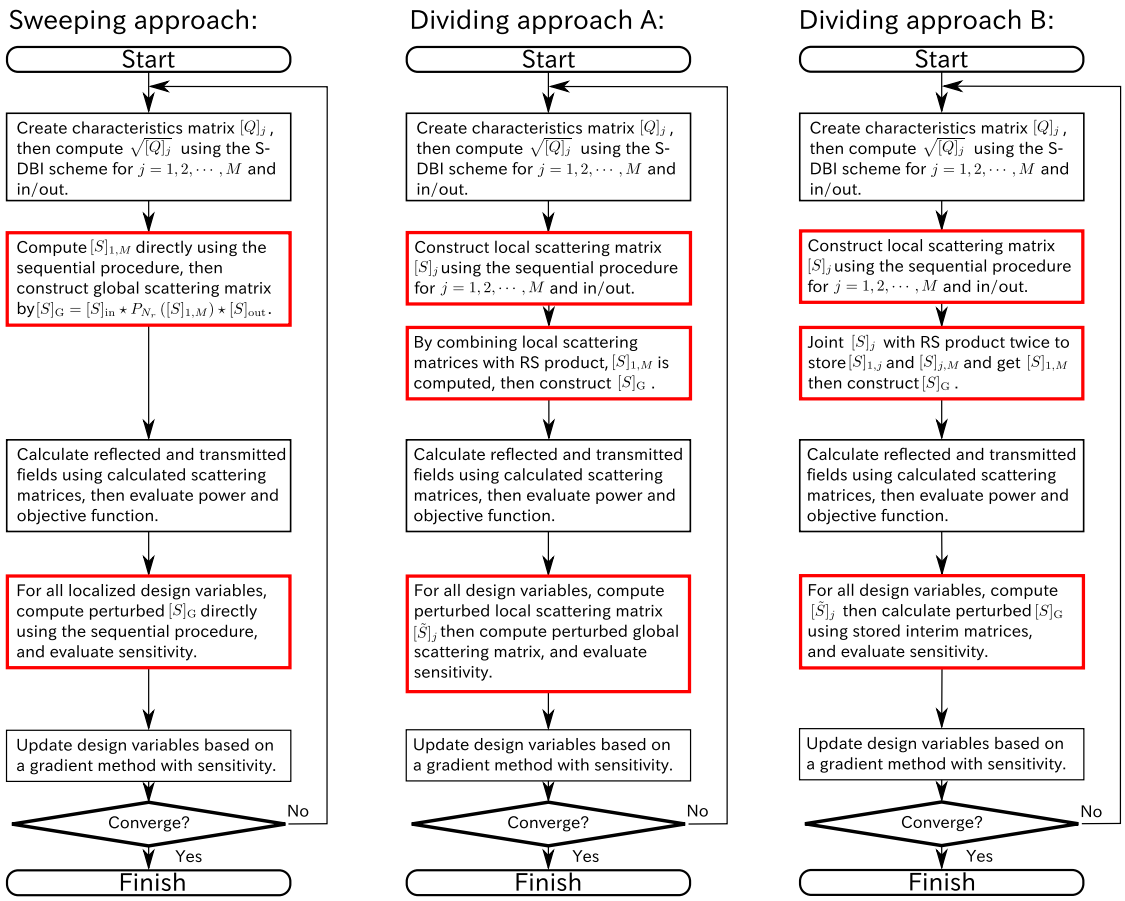

Fig. 3. Flow charts of structural optimization based on sensitivity analysis with the sweeping approach, the dividing approach A, and B.

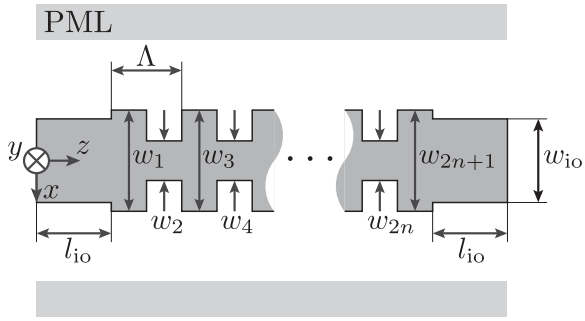

Fig. 4. A design schematic of a reflector based on a waveguide grating.

We compare the three design approaches in terms of average elapsed time of one iteration in structural optimization. Figure 6 shows the elapsed time as a function of the number of layers, $M = 2n + 1$. Throughout this paper, we use a PC with Intel Xeon CPU E5-2660 v4 @ 2.00 GHz. One can see that the dividing approach B is the least time consumption of the three. It may be useful for shape optimization because the differences are significant especially for optimization with relatively a large number of design variables.

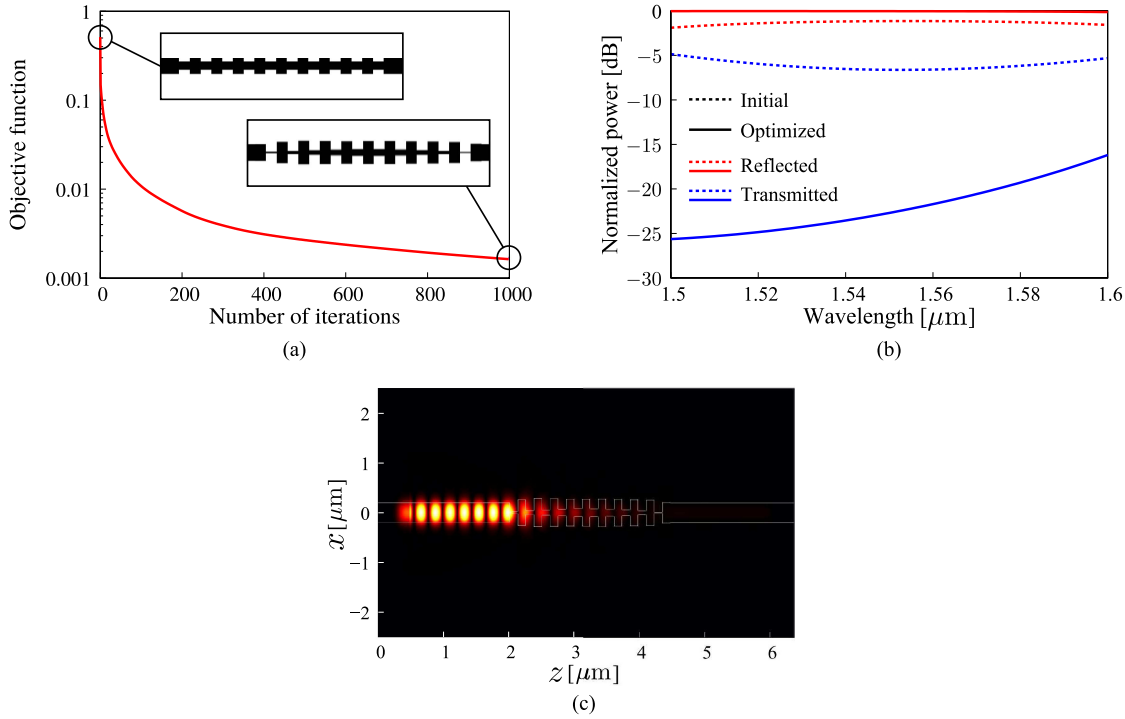

Fig. 5. Optimization results of the waveguide reflector when $M = 21$ ($n = 10$). (a) The objective function as a function of iteration number. (b) Transmission and reflection spectra of the initial and optimized reflector. (c) Propagation field in the optimized reflector simulated by the FDTD at wavelength of 1.55 μm.

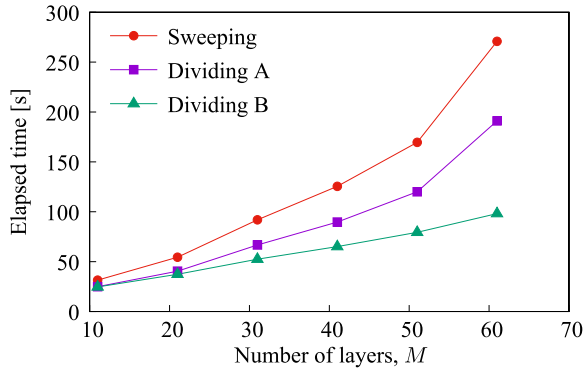

Fig. 6. Average elapsed time of one iteration in structural optimization of the waveguide reflector as a function of the number of layers, $M = 2n + 1$.

3.2. Polarizer Based on 1-D Photonic Crystal

Next, shape optimization of a polarizer based on 1-D photonic crystal (PhC) is conducted. The design schematic is shown in Fig. 7. In this example, one period of 1-D PhC is optimized so that the TE_0 mode (TM-like wave in 3-D waveguides) is output into through port and TM_0 is shut off. The refractive index of Si core surrounded by SiO_2 is determined approximately by an effective index

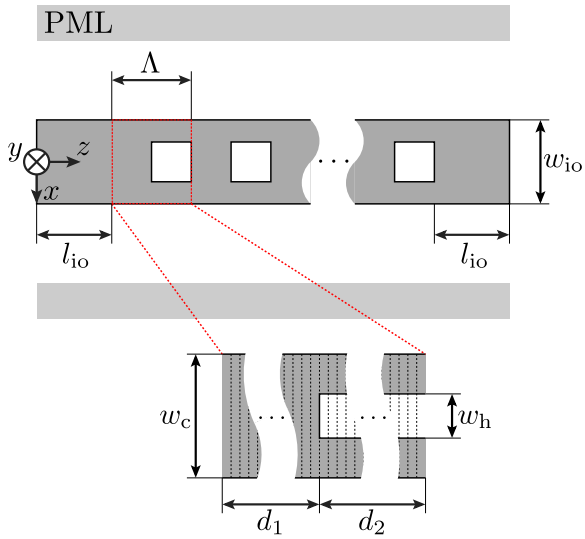

Fig. 7. Design schematic of a polarizer based on 1-D photonic crystal.

method assuming 250 nm core height. The objective function is let to be as follows:

$$\underset{\{a\}}{\text{minimize}} \quad f(\{a\}) = \sum_{\lambda \in \{L\}} \left\{ f_{\text{TE0}}(\{a\}, \lambda) + W f_{\text{TM0}}(\{a\}, \lambda) \right\} \tag{24}$$

with

$$f_{\text{TE0}}(\{a\}, \lambda) = \left\{ 1 - P_{\text{TE0,thru}}(\{a\}, \lambda) \right\}^2 \tag{25}$$

$$f_{\text{TM0}}(\{a\}, \lambda) = \left\{ 0 - \frac{P_{\text{TM0,thru}}(\{a\}, \lambda)}{P_{\text{TM0,refl}}(\{a\}, \lambda)} \right\}^2 \tag{26}$$

where $P_{\text{T}X\text{,thru}}$ and $P_{\text{T}X\text{,refl}}$ are normalized power of T$X \in \{\text{TE}_0, \text{TM}_0\}$ mode at through and input ports when TX mode is launched into input port. W is a weight, and it is taken to be 100 so as to maintain < -20 dB transmission of TM wave. A set of wavelengths is $\{L\} = \{1.53,\ 1.5475,\ 1.565\ \mu\text{m}\}$ to achieve wavelength-flattened operation at C-band. The other structural parameters shown in Fig. 7 are let to be as follows: $w_{\text{io}} = 450$ nm, $l_{\text{io}} = 100$ nm, $\Lambda = 360$ nm ($d_1 = 210$ nm, $d_2 = 150$ nm). In the initial profile, $w_{\text{c}} = 450$ nm and $w_{\text{h}} = 170$ nm. One period is divided into M layers in $z-$direction, and we let $\Lambda/M = 10$ nm. Design variables are core widths and hole sizes at each divided layer, that is, the number of design variables is 51. Transversal computational window size including 500 nm PML is 5 μm, and the number of sampling points is 250.

The optimization results when the number of periods, N_r, is 10 are shown in Fig. 8. Figure 8 (a) is the objective function as a function of iteration number, and the insets are an initial profile and an optimized profile after 300 iteration. Transmittance spectra at the through port and propagating wave computed by the FDTD are shown in Fig. 8 (b) and (c). Compared with an initial profile, higher TE-wave transmission ($>$ 96%) and lower TM-wave transmission (< -25 dB) is achieved at shown range, C-band.

Three design approaches in terms of average elapsed time of one iteration are compared by changing N_r. Figure 9 shows the elapsed time as a function of N_r. Also in this comparison, the dividing approach B is the least time consumption of the three not depending on N_r. Thus, this design approach has potential that photonic devices with periodicity can be efficiently optimized.

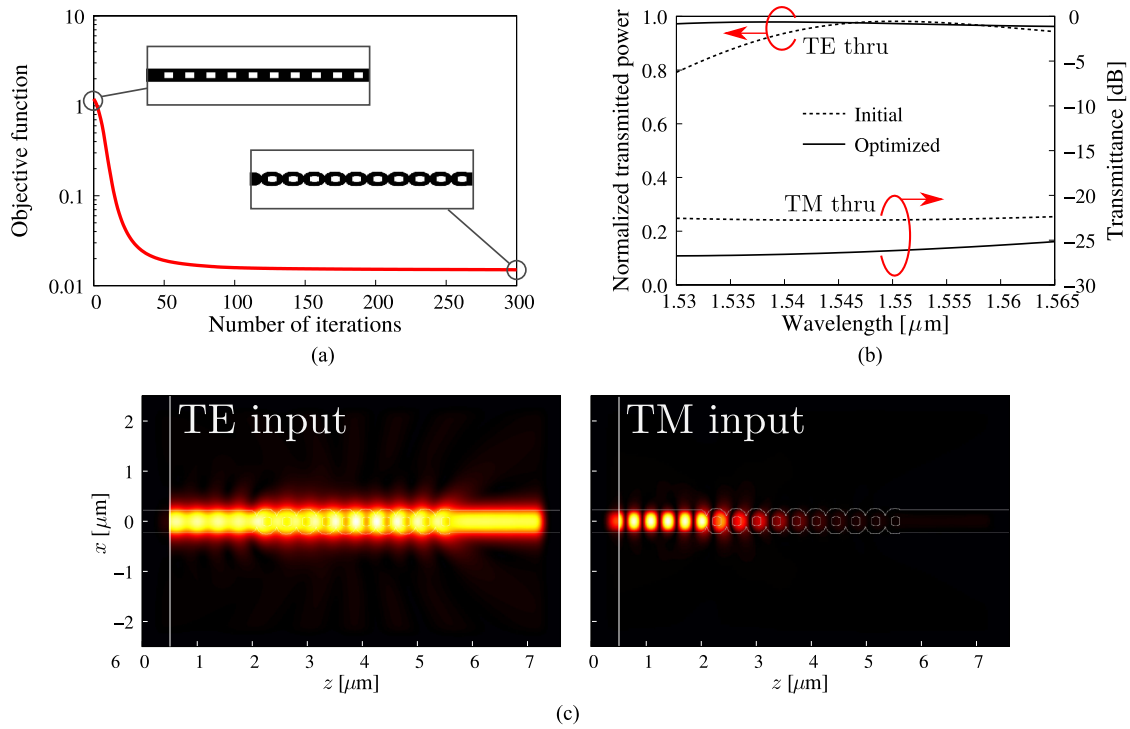

Fig. 8. Optimization results of the polarizer when $N_r = 10$. (a) The objective function as a function of iteration number. (b) Transmission spectra at the through port of the initial and optimized reflector. (c) Propagation field in the optimized polarizer simulated by the FDTD at wavelength of 1.5475 μm.

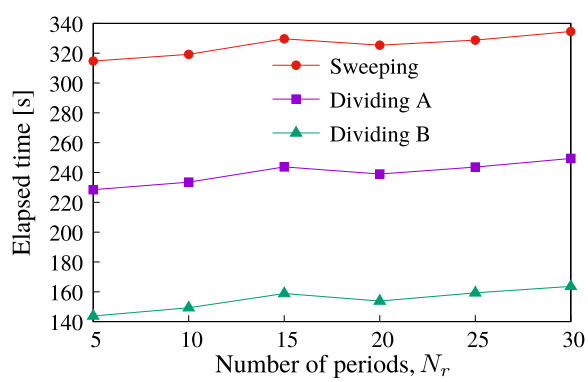

Fig. 9. Average elapsed time of one iteration in structural optimization of the polarizer based on periodic 1-D PhC as a function of N_r.

IV. Conclusion

In this paper, we presented structural optimization based on the SO-Bi-BPM and sensitivity analysis for design of photonic integrated components in high-index-contrast waveguides. Three design approaches using characteristics of scattering operator are presented and compared by optimal design of the waveguide reflector and the polarizer based on 1-D PhC. It is found out that the dividing approach, where the global scattering matrix are divided into local scattering matrices and interim matrices of RS product are stored, is the most efficient in terms of elapsed time of one iteration in structural optimization. Our design approach can be contributed to efficient structural optimization with high design of freedom especially for photonic devices with periodicity.

References

[1] B. Jalali and S. Fathpour, "Silicon photonics," *J. Lightw. Technol.*, vol. 24, no. 12, pp. 4600–4615, Dec. 2006.
[2] D. Gramotnev and S. Bozhevolnyi, "Plasmonics beyond the diffraction limit," *Nat. Photon.*, vol. 4, no. 2, pp. 83–91, Jan. 2010.
[3] J. S. Jensen and O. Sigmund, "Systematic design of photonic crystal structures using topology optimization: Low-loss waveguide bends," *Appl. Phys. Lett.*, vol. 84, no. 12, pp. 2022–2024, Mar. 2004.
[4] Y. Tsuji, K. Hirayama, T. Nomura, K. Sato, and S. Nishiwaki, "Design of optical circuit devices based on topology optimization," *IEEE Photon. Technol. Lett.*, vol. 18, no. 7, pp. 850–852, Apr. 2006.
[5] J. Lu and J. Vucković, "Nanophotonic computational design," *Opt. Express*, vol. 21, no. 11, pp. 13351–13367, Jun. 2013.
[6] R. Matzen, J. S. Jensen, and O. Sigmund, "Systematic design of slow-light photonic waveguides," *J. Opt. Soc. Amer. B*, vol. 28, no. 10, pp. 2374–2382, Oct. 2011.
[7] L. H. Frandsen *et al.*, "Topology optimized mode conversion in a photonic crystal waveguide fabricated in silicon-on-insulator material," *Opt. Express*, vol. 22, no. 7, pp. 8525–8532, Apr. 2014.
[8] M. A. Swillam, M. H. Bakr, and X. Li, "Full vectorial 3-D sensitivity analysis and design optimization using BPM," *J. Lightw. Technol.*, vol. 26, no. 5, pp. 528–536, Mar. 2008.
[9] Y. Nito, J. Shibayama, J. Yamauchi, and H. Nakano, "Full-vectorial beam-propagation methods based on a fundamental scheme–Design of a short polarization converter," *J. Lightw. Technol.*, vol. 32, no. 21, pp. 4111–4118, Nov. 2014.
[10] A. Iguchi, Y. Tsuji, T. Yasui, and K. Hirayama, "Topology optimization of optical waveguide devices based on beam propagation method with sensitivity analysis," *J. Lightw. Technol.*, vol. 34, no. 18, pp. 4214–4220, Sep. 2016.
[11] A. Iguchi, Y. Tsuji, T. Yasui, and K. Hirayama, "Efficient topology optimization of optical waveguide devices utilizing semi-vectorial finite-difference beam propagation method," *Opt. Express*, vol. 25, no. 3, pp. 28210–28222, Nov. 2017.
[12] A. Iguchi, Y. Tsuji, T. Yasui, and K. Hirayama, "Efficient shape and topology optimization based on sensitivity analysis for optical waveguide devices utilizing full-vectorial BPM," *J. Lightw. Technol.*, vol. 38, no. 8, pp. 2328–2335, Apr. 2020.
[13] H. -P. Nolting and G. Sztefka, "Eigenmode matching and propagation theory of square meander-type couplers," *IEEE Photon. Technol. Lett.*, vol. 4, no. 12, pp. 1386–1389, Dec. 1992.
[14] P. Bienstman and R. Baets, "Optical modelling of photonic crystals and VCSELs using eigenmode expansion and perfectly matched layers," *Opt. Quant. Electron.*, vol. 33, no. 4, pp. 327–341, Apr. 2001.
[15] R. Pregla, *Analysis of Electromagnetic Fields and Waves: The Method of Lines*. Hoboken, NJ, USA: Wiley, 2008.
[16] H. Liang, J. Mu, R. A. Soref, X. Li, and W. Huang, "An optical mode-matching method with improved accuracy and efficiency," *IEEE J. Quantum Electron.*, vol. 51, no. 2, Feb. 2015, Art. no. 6100108.
[17] H. Rao, R. Scarmozzino, and R. M. Osgood, "A bidirectional beam propagation method for multiple dielectric interfaces," *IEEE Photon. Technol. Lett.*, vol. 11, no. 7, pp. 830–832, Jul. 1999.
[18] S. Wu and J. Xiao, "An efficient semivectorial bidirectional beam propagation method for 3-D optical waveguide structures," *J. Lightw. Technol.*, vol. 34, no. 4, pp. 1313–1321, Feb. 2016.
[19] P. L. Ho and Y. Y. Lu, "A stable bidirectional propagation method based on scattering operators," *IEEE Photon. Technol. Lett.*, vol. 13, no. 12, pp. 1316–1318, Dec. 2001.
[20] P. L. Ho and Y. Y. Lu, "A bidirectional beam propagation method for periodic waveguides," *IEEE Photon. Technol. Lett.*, vol. 14, no. 3, pp. 325–327, Mar. 2002.
[21] A. M. A. Said, A. M. Heikal, N. F. F. Areed, and S. S. A. Obayya, "Why do field-based methods fail to model plasmonics?," *IEEE Photon. J.*, vol. 8, no. 5, Oct. 2016, Art. no. 4802613.
[22] H. A. Jamid and M. Z. M. Khan, "A numerical approach for full-vectorial analysis of 3-D guided wave structures with multiple and strong longitudinal discontinuities," *IEEE J. Quantum Electron.*, vol. 45, no. 2, pp. 117–124, Feb. 2009.
[23] J. Yamauchi, M. Sekiguchi, O. Uchiyama, J. Shibayama, and H. Nakano, "Modified finite-difference formula for the analysis of semivectorial modes in step-index optical waveguides," *IEEE Photon. Technol. Lett.*, vol. 9, no. 7, pp. 961–963, Jul. 1997.
[24] N. J. Higham, "Stable iterations for the matrix square root," *Numer. Algorithms*, vol. 15, no. 2, pp. 227–242, Sep. 1997.
[25] C. Moler and C. V. Loan, "Nineteen dubious ways to compute the exponential of a matrix, twenty-five years later," *SIAM Rev.*, vol. 45, no. 1, pp. 3–49, 2003.
[26] J. Corones and R. Krueger, "Obtaining scattering kernels using invariant imbedding," *J. Math. Anal. Appl.*, vol. 95, no. 2, pp. 393–415, Sep. 1983.
[27] L. Yuan and Y. Y. Lu, "A recursive-doubling Dirichlet-to-Neumann-map method for periodic waveguides," *J. Lightw. Technol.*, vol. 25, no. 11, pp. 3649–3656, Nov. 2007.
[28] H. H. Li, "Refractive index of silicon and germanium and its wavelength and temperature derivatives," *J. Phys. Chem. Ref. Data*, vol. 9, no. 3, pp. 561–658, 1980.
[29] C. Z. Tan, "Determination of refractive index of silica glass for infrared wavelengths by IR spectroscopy," *J. Non-Cryst. Solids*, vol. 223, no. 1, pp. 158–163, Jan. 1998.